Ultra-Stable Atmospheric Short Link for the Optical Frequency Signal Transfer

Vishnyakova G. A.[1], Kudeyarov K. S.[1], Chiglintsev E. O.[2], Zhadnov N. O.[1], Kryuchkov D. S.[1], Khabarova K. Yu.[1], Kolachevsky N. N.[1,2]

[1]P.N. Lebedev Physical Institute of the Russian Academy of Sciences, Moscow, Russia
[2]Russian Quantum Center, Moscow, Russia
e-mail: gulnarav7@gmail.com

***Abstract*—The 17 m open-air link for coherent transfer of ultrastable optical frequency signal have been demonstrated. The fractional frequency instability caused by air turbulence is suppressed by more than 3 orders of magnitude with the help of active noise compensation system and reaches $1.7 \cdot 10^{-19}$ after averaging time of 1000 s. The link contribution to uncertainty is decreased by more than 400 times and is equal to $5 \cdot 10^{-20}$.**

Keywords—Allan deviation, power spectral density, phase noise, optical frequency transfer, atmospheric turbulence, autoheterodyning scheme

I. INTRODUCTION

The best state-of-the-art optical frequency standards based on cold atoms and ions possess the relative uncertainty and instability at the level of low 10^{-18} [1,2]. The global network of optical clocks cooperated by the ultrastable links [3] create new perspectives in such fields of science and technology as the satellite navigation, time scales formation, very-long-baseline interferometry, relativistic geodesy, tests of fundamental theories, search for fundamental constants drift and dark matter, etc. The radio frequency transfer techniques cannot maintain the 10^{-18} level of inaccuracy and instability [4] whereas the transfer using optical carrier over the links with active phase noise compensation does. The rapid development of stationary and transportable [5] optical clocks shows the necessity of developing both fiber [6,7] and open-air [8] links for the ultrastable signals transfer.

Here we report on our recent progress in developing open-air atmospheric link for the transfer of ultrastable frequency signal at 1.5 μm. The 17 m open-air link including active angle-of-arrival stabilization and phase noise compensation systems has been demonstrated.

II. EXPERIMENTAL SETUP

The optical signal travelling through an open-air link suffers from atmospheric turbulence which causes phase noise as well as intensity fluctuations called scintillations [9], angle-of-arrival jitter and waviness of the phase front [10]. The latter sets the maximum useful beam diameter called Fried parameter [11] competing with the necessity of expanding the beam for decreasing of the diffraction divergence.

The power spectral density (PSD) of the phase noise induced by the fluctuations of air refractive index is described by the Kolmogorov theory of turbulence [12]:

$$S_\phi(f) = 0.016 \cdot k^2 \cdot C_n^2 \cdot L \cdot V^{5/3} \cdot f^{-8/3}, \qquad (1)$$

where f is Fourier frequency, k is the wave number of light, C_n^2 is the atmospheric turbulence structure constant, L is the free-space link length, and V is the wind speed.

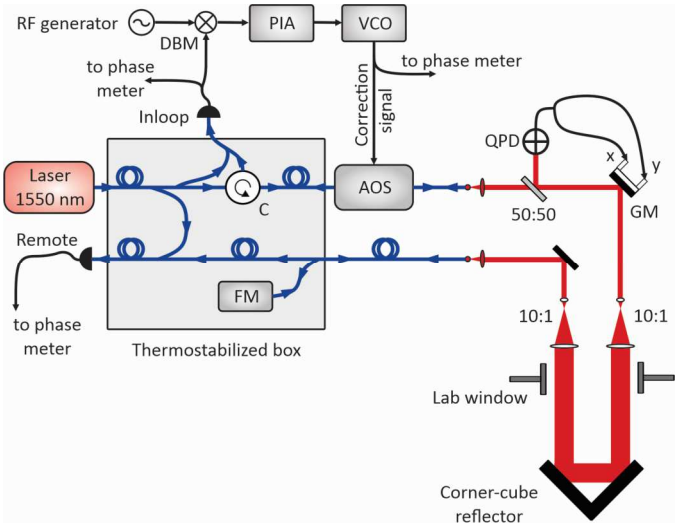

Fig. 1. The simplified experimental setup. C – optical circulator, AOS – acousto-optical shifter, 50:50 – beam splitter, QPD – quadrant photodetector, GM – 2D galvo mirror, 10:1 – Keplerian telescope, FM – Faraday mirror, DBM – double balanced mixer, RF – radio-frequency, PIA – proportional-integral amplifier, VCO – voltage-controlled oscillator. Blue lines stand for optical fibers, red lines – for optical beams in free-space and black lines – for electric signals.

The operating wavelength has been chosen to be 1.5 μm since both standard optical fibers and air have transparency window in this spectral range; there exist reliable Er-doped fiber amplifiers and fiber lasers including femtosecond ones; the best ultrastable laser systems based on monocrystalline silicon cavities work at this frequency [13]. The principle experimental setup is shown in the Fig. 1. The main parts of the open-air link ultrastable frequency transfer scheme are the system of phase noise detection and cancellation and the system of beam expansion and angle-of-arrival stabilization. The all-fiber thermostabilized autoheterodyning scheme is used for

978-1-6654-3935-0/21/$31.00 ©2021 IEEE

measuring and compensating the phase fluctuations introduced by the atmospheric turbulence. The radiation at 1550.12 nm (ITU Channel 34) from the fiber laser Koheras AdjustIK E15 is split into 3 parts: the first one is sent into the link via an acousto-optical shifter (AOS), the second one is the local arm for the inloop beat signal used for error signal formation at the sender site and the third one is the local arm for the remote (i.e. delivered to the remote receiver) beat signal used for the full characterization of the link performance. At the receiver site (which co-locates with the sender to allow for remote beat note creation) the light is partially reflected by Faraday mirror (FM) and after passing the link in the opposite direction forms the inloop beat note detected by the InGaAs photodiode. This beat signal is demodulated at the double balanced mixer (DBM) by the reference signal from the radio-frequency (RF) generator at frequency ν_{RF} and then is sent to proportional-integral amplifier (PIA) which in turn governs the frequency of the voltage-controlled oscillator (VCO) driving AOS. Thereby the AOS frequency (correction signal) adapts in a way to compensate for the link phase noise. To extract the instability, inaccuracy and PSD characterizing the link we record inloop, remote and correction signals by a high-resolution dead-time-free phase recorder K+K Messtecknik [14] referenced by the aforementioned RF generator. Each of 3 signals are recorded by pair of independent K+K channels to detect cycle-slip events [15].

After passing the fiber-coupled AOS the beam is collimated to the free space and expanded by 10 times with the telescope in Keplerian configuration. To form 17 m atmospheric link the beam is sent through the lab window to the corner-cube reflector (CCR) attached 8.5 meters away. The beam is adjusted to return to the lab being horizontally shifted by CCR and then after passing the separate telescope is coupled into the fiber. To stabilize the angle-of-arrival we use quadrant photodetector (QPD) and 2D tip-tilt galvo mirror (GM). The mirror should be located at the conjugate telescope point to prevent the conversion of tip/tilt to displacement jitter [10].

III. RESULTS AND DISCUSSION

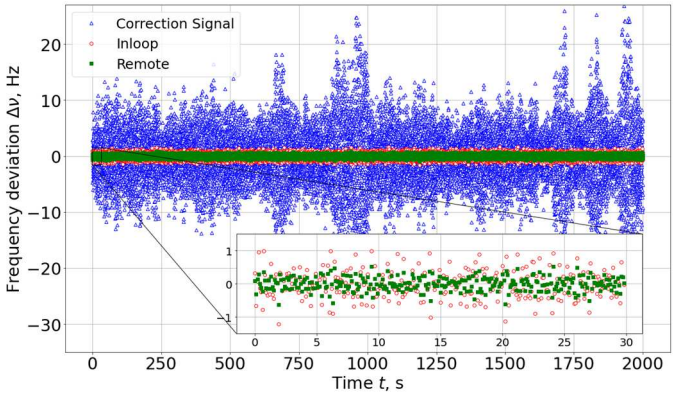

Fig. 2. Frequency deviation versus time for correction (blue empty triangles), inloop (red empty circles) and remote (green filled squares) signals recorded with 100 ms time window of phase meter in "Phase" mode. The target value of signal frequency (ν_{RF} for inloop and $\nu_{RF}/2$ for remote and correction) has been subtracted for clearness. The inset shows the portion of inloop and remote data in details.

We have succeeded to obtain more than 11 000 seconds of continuous data. Typical time dependences of frequency and phase fluctuations recorded using 100 ms measuring window of phase meter are shown in Fig. 2 and 3 for inloop, remote and correction signals. The mode of phase meter was set to be "Phase" that corresponds to Π-mode. It is clearly seen that the feedback loop dramatically suppresses frequency and phase excursions. For analyzing frequency instability for times less than 100 ms and phase noise PSD for Fourier frequencies greater than 5 Hz we have additionally recorded 550 seconds of data with 1 ms phase meter window.

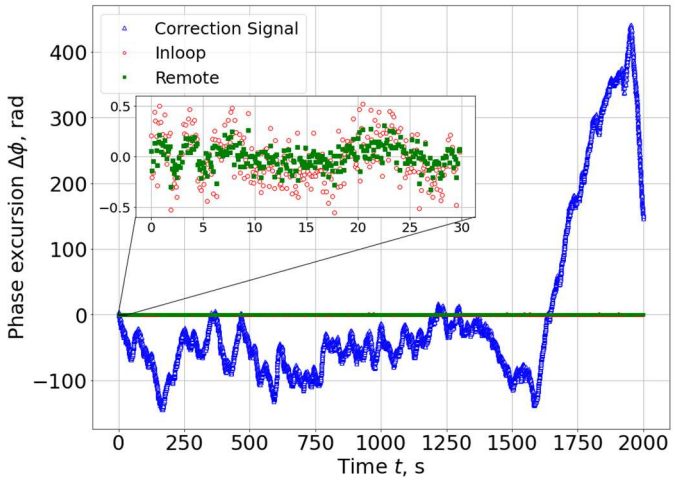

Fig. 3. Phase deviation versus time for correction (blue empty triangles), inloop (red empty circles) and remote (green filled squares) signals recorded with 100 ms time window of phase meter in "Phase" mode. The linear slope corresponding to target frequency (ν_{RF} for inloop and $\nu_{RF}/2$ for remote and correction) has been subtracted for clearness. The inset shows the portion of inloop and remote data in details.

The fractional frequency instability in terms of Allan deviation is shown in the Fig. 4. The values for averaging times less than 100 ms are calculated from 1 ms time window data set. Active noise compensation system allows us to reduce the instability by more than 3 orders of magnitude from $2.6 \cdot 10^{-16}$ for correction signal to $1.7 \cdot 10^{-19}$ for remote at averaging time τ = 1000 s. The link contribution to inaccuracy of transferred signal (that is the difference between actual mean frequency and target one) is reduced from $1.9 \cdot 10^{-17}$ to $5 \cdot 10^{-20}$. The slope of Allan deviation for inloop is τ^{-1} that corresponds to flicker phase, white phase or higher order noise type [15]. To extract the noise type we also analyzed the modified Allan deviation which has the $\tau^{-3/2}$ slope that points to the domination of the white phase noise and proves the correct operation of the feedback loop. The deviation of remote is 2 times smaller than the one of inloop which means that it is limited by the electronic noise floor but not by the delay-unsuppressed noise (DUN) of the link which will be discussed later.

The PSD of phase fluctuations is plotted in the Fig. 5. There are pronounced resonant peaks at the frequencies larger than 5 Hz that most probably correspond to acoustic vibrations. The 60 mHz – 1 Hz frequency region has the slope of $f^{-8/3}$ in accordance with Kolmogorov spectrum.

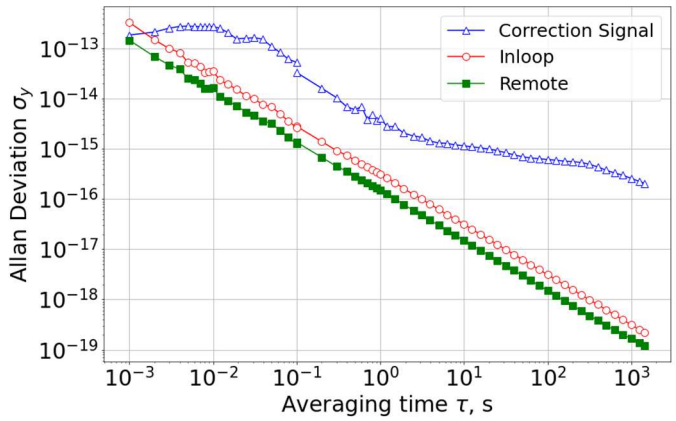

Fig. 4. Allan deviation versus averaging time for correction (blue empty triangles), inloop (red empty circles) and remote (green filled squares) signals. Markers are connected by lines for eye guidance.

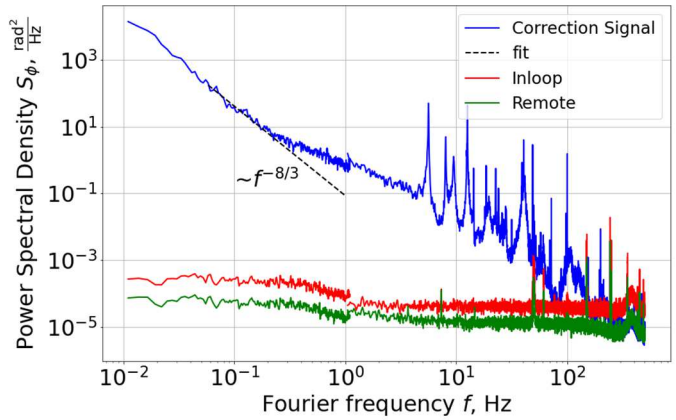

Fig. 5. Power spectral density of phase fluctuations versus Fourier frequency for correction signal (blue upper curve), inloop (red middle curve) and remote (green lower curve). Dashed black line is the power law approximation of the selected region of correction signal.

For very long links the fundamental limit for the values of instability and PSD is imposed by the delay-unsuppressed noise [15]. For our short link DUN calculated from the correction signal phase noise PSD is less than 10^{-13} rad^2/Hz for $f < 2$ Hz and less than 10^{-9} rad^2/Hz in the resonant region ($f > 5$ Hz) that is several orders of magnitude less than the obtained remote phase noise PSD and does not limit the instability.

Further steps will be the increase of the link length up to 500 m and the use an unmanned aerial vehicle with a corner-cube reflector fixed on it as a moving receiver model.

IV. Conclusions

We have demonstrated the frequency transfer over atmospheric short 17 m link. The setup includes the systems for compensation of angle-of-arrival fluctuations and suppression of phase noise caused by air turbulence. The obtained values for link contribution to instability and inaccuracy of transferring signal are suitable for the precision experiments like clock comparison or chronometric levelling.

Acknowledgment

This work is supported by the Russian Science Foundation (Grant No. 19-72-10166).

References

[1] E. Oelker, R. B. Hutson, C. J. Kennedy, L. Sonderhouse, T. Bothwell, A. Goban, et al., "Demonstration of 4.8×10^{-17} stability at 1 s for two independent optical clocks", Nat. Photonics 13, 714–719 (2019)

[2] S. M. Brewer, J.-S. Chen, A. M. Hankin, E. R. Clements, C. W. Chou, D. J. Wineland, et al., "$^{27}Al^+$ quantum-logic clock with a systematic uncertainty below 10^{-18}", Phys. Rev. Lett., 123, 033201 (2019)

[3] F. Riehle, Nat. Photonics, 11, 25 (2017)

[4] M. Fujieda, D. Piester, T. Gotoh, J. Becker, M. Aida, and A. Bauch, "Carrier-phase two-way satellite frequency transfer over a very long baseline", Metrologia 51, 253 (2014)

[5] S. B. Koller, J. Grotti, St. Vogt, A. Al-Masoudi, S. Dörscher, S. Häfner, et al., "Transportable optical lattice clock with 7×10^{-17} uncertainty", Phys. Rev. Lett., 118 (7), 073601 (2017)

[6] G. Grosche, O. Terra, K. Predehl, R. Holzwarth, B. Lipphardt, F. Vogt, et al., "Optical frequency transfer via 146 km fiber link with 10^{-19} relative accuracy", Optics Letters 34, 2270 (2009)

[7] S. Droste, T. Udem, R. Holzwarth, T. W. Hänsch, "Optical frequency dissemination for metrology applications", Compt. Rend. Phys., 16 (5), 524 (2015)

[8] D. R. Gozzard, L. A. Howard, B. P. Dix-Matthews, S. F. E. Karpathakis, C. T. Gravestock, and S. W. Schediwy, "Ultra-stable free-space laser links for a global network of optical atomic clocks", arXiv:2103.12909 (2021)

[9] M. Grabner, V. Kvicera,"Measurement of the structure constant of refractivity at optical wavelengths using a scintillometer", Radioengineering, 21, 1, 455-458 (2012)

[10] W. C. Swann, L. C. Sinclair, I. Khader, H. Bergeron, J.-D. Deschênes, and N. R. Newbury, "Low-loss reciprocal optical terminals for two-way time-frequency transfer", Appl. Opt., 56, 9406 (2017)

[11] D. L. Fried, "Optical heterodyne detection of an atmospherically distorted signal wave front", Proc. IEEE, 55, 57-67 (1967)

[12] L. C. Sinclair, F. R. Giorgetta, W. C. Swann, E. Baumann, I. Coddington, and N. R. Newbury, "Optical phase noise from atmospheric fluctuations and its impact on optical time-frequency transfer", Phys. Rev. A, 89, 023805 (2014)

[13] D. G. Matei, T. Legero, S. Häfner, C. Grebing,, R. Weyrich, W. Zhang, et al., "1.5 μm lasers with sub-10 mHz linewidth", Phys. Rev. Lett., 118 (26), 263202 (2017)

[14] G. Kramer, and W. Klische, "Multi-channel synchronous digital phase recorder", Proceedings of the 2001 IEEE International Frequncy Control Symposium and PDA Exhibition (Cat. No.01CH37218), 144–151 (2001)

[15] S. Droste, "Optical frequency transfer via telecommunication fiber links for metrological application", PhD thesis, Leibniz Universitat Hannover, (2014)